





Dual-Linear-Polarized X-Slot Sub-Array for Sub-6GHz 5G Applications

Husam.H.AL-Naqeeb^{1*}  Mohammad J. Namaazi¹  Hadi Aliakbarian¹  Faris Muhammed Ali² 

Received: 8th May 2025 / Accepted: 3rd August 2025 / Published Online: 1st December 2025

© The Author(s), under exclusive license to the University of Thi-Qar

Abstract

Dual linear polarized cross-slot patch antenna is a good candidate for modern base station antennas in sub-6 GHz fifth-generation (5G) cellular communications due to its low profile, low cost and moderate bandwidth. The best-obtained results of the single antenna design demonstrate a wide impedance bandwidth of 19.72% (3.2–3.9 GHz) for VSWR < 1.4, isolation of less than 50 dB between both ports, and a high gain of 10.5 dBi. The designed dual-polarized antenna was placed in a two-element array that is formed once with and once without via pins in two cases: 1- vertical/horizontal polarization. 2- $\pm 45^\circ$ slant polarization. The radiation pattern in both incidents has been studied and reported. In case one, the results show that the mutual coupling deteriorates the radiation pattern with the side lobe of around -12.6 dB at 3.4 GHz. However, the sidelobe level is better at the level of -19 dB, although not acceptable in the case of square vias. The S11 is good from 3.25 GHz to 3.7 GHz (450 MHz). Similarly, the gain is 13.5 dBi without a via and with a via. A great result: an increase from 10.5 dBi for a single element to 13.5 dBi for a two-antenna array. In case two, the best result obtained in this scenario is that the S11 is below -10 dB from 3.2 to 3.9 (700 MHz) without the use of vias. The 45-degree slant radiation patterns of the antenna, which are plotted in both perpendicular radiations. Both co-polar and cross-polar patterns are shown and are overlaid. The VSWR is less than 1.5 in all cases. The results obtained and the compatibility achieved in this direction allow for the possibility of using this antenna in many applications in modern communications systems, such as advanced antenna systems (AAS) and radars.

Keywords— Array antenna, Dual-polarized, Base station antenna, Microstrip patch antenna, High isolation, Cross slot, 5G.

1 Introduction

Antenna design for 5th generation (5G) cellular communication has been one of the key parts of important research topics in the antenna community (Asplund et al., 2020). There is a considerable amount of published research related to the antennas used on both the base station side and the terminal side of 5G networks (Muirhead et al., 2016). Many significant advancements in 5G technology have been made for the base station to boost high data rates and bandwidth, including massive MIMO (multiple input, multiple output), beamforming capabilities, network densification, low latency, and energy efficiency. Among various designs

*Husam H. Al-Naqeeb

hadihussam3@gmail.com

Mohammad Javaad Namaazi

mohammadjavaad.namaazi@email.kntu.ac.ir

Hadi Aliakbarian

aliakbarian@eetd.kntu.ac.ir

Faris Muhammed Ali

faris@atu.edu.iq

¹ Faculty of Electrical Engineering, KN Toosi Univ. of Technology, Tehran, Iran Affiliation

² Department of Communications Techniques Engineering, Engineering Technical College Najaf, Al-Furat Al-Awsat Technical University, Najaf, Iraq

reported for base station antennas, antennas with dual polarization are preferred due to the necessity of using polarization diversity in such antennas. Among different dual-polarized configurations, dual-slant designs are mostly preferred due to their symmetrical pattern in both vertical and horizontal planes. Dual polarization enhances spectral efficiency and provides polarization diversity, which in turn improves signal robustness and resilience to interference. (Vaziri et al., 2013; Chen & Vaughan, 2013).

Various approaches to dual-polarization antennas have been developed to meet these requirements, as described in (Gao et al., 2003; Huang et al., 2009). Many works have used an aperture-coupled feed to improve bandwidth and isolation (Gao et al., 2003; Guo et al., 2021). Some of them have used an aperture-coupled L probe fed together (Joo Seong Jeon, 2011). Others used a coaxial feed and printed dipoles (Biao Li et al., 2012; Huang et al., 2009). An array antenna base station uses baluns to provide balanced feed and impedance matching to these elements (Sun et al., 2019; Zhang & Gao, 2018). Incorporating spiral-choked LB elements into the dual-band antenna array enhances both bandwidth and isolation within the high band. The spiral chokes contribute to widening the bandwidth of the choked LB antenna, thereby extending its operational frequency range (Sun et al., 2020; Sun et al., 2020). Varactor diodes have been used to activate continuous null scanning, beam steering, and pattern reconfiguration (Ding et al., 2021; Zhang et al., 2023). A patch antenna with an aperture-coupled design is suitable for sub-6 GHz and high 5G applications (Azari et al., 2023; Azari et al., 2024).

All of these methods make it difficult to use as a modern base station. The reflector included in the antenna design provides various positive uses, including directed radiation when the reflector, which is somewhat larger than the ground plane, aids in creating directional radiation patterns. By managing the reflection of transmitted signals, the antenna can direct its energy in certain directions, improving its directivity, gain, and radiation pattern (Guo et al., 2021).

The crossed-slot design generates dual linear polarizations by crossing the slots at orthogonal angles; the antenna can transmit or receive signals with both perpendicular polarizations, allowing for polarization diversity in modern base station communication systems. Crossed-slot antennas have the advantage of providing a wider bandwidth than other low-profile antenna layouts. The crossed-slot construction enables broad frequency coverage, making it suited for applications that need wideband operation. As a result, the crossed-slot antenna design was chosen due to its ability to provide polarization diversity, wideband operation, low profile, cost-effectiveness, large bandwidth, and improved isolation characteristics, making it an appropriate choice for applications requiring high-performance dual-polarized antennas in 5G base station applications.

The goal of this paper is to introduce an improved crossed-slot element antenna and subarray design with a simple feed mechanism that achieves strong polarization isolation over a wide bandwidth. The main idea of the antenna element used in this work came from (Vaziri et al., 2013), while the design has been completely changed to fit the 5G base station requirements. The antenna arrangement feeds the slots with symmetric microstrip lines, efficiently suppressing mutual coupling. This design removes the requirement for parasitic patches, usually employed in dual-polarized antennas, resulting in a broader bandwidth and a simpler overall structure. The antenna performs well in gain, impedance bandwidth, feed isolation, and polarization purity, making it appropriate for polarization diversity, satellite communications, and polarimetric radar.

The rest of the paper is organized as follows: In Section 2, the design of a single-element antenna is presented. In Section 3, we will discuss the issue of ground radiation, its causes, mathematical analysis, and methods of solving it. In Section 4, a two-element sub-array design of the antenna is presented for 5G base station applications.

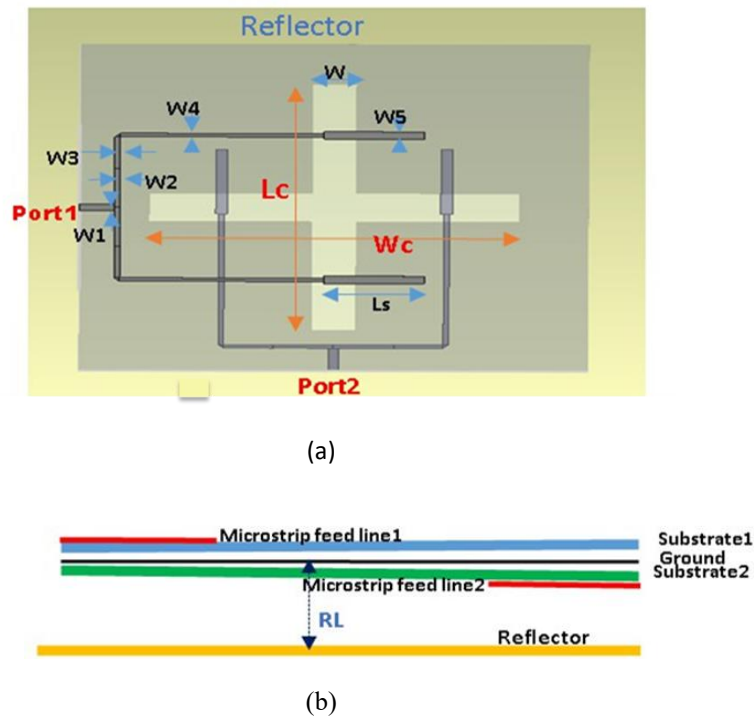


Figure 1: Proposed single antenna geometry with labeled design parameters (a) top view and (b) side view

2 Single Element Cross-Slot Design

2.1 Element Configuration

Assuming that we need to design a reflector-backed cross-slot antenna with an operating bandwidth from 1 to 4 GHz and a center frequency of 3.5 GHz, $\lambda_0/4=21.21\text{mm}$, and $\epsilon_r = 3.55$. The substrate is chosen as Rogers RO4003C. The proposed antenna has two layers: the first serves as a reflector, while the second comprises two microstrip lines, two substrates, a ground plane, and a cross-slot aperture (Vaziri et al., 2013-Chen & Vaughan, 2013).

The structure of the proposed antenna element is shown in Figure 1. As can be seen, microstrip lines are employed to enable balanced feeding of slots on opposing sides of the ground plane. This type of feeding, let us call it balanced feeding, helps to reduce reciprocal coupling between the slots and their feeding lines, resulting in better polarization separation and purity. Microstrip lines are relatively easy to design and implement, making them a viable option for feeding antenna slots. The simple design of microstrip lines adds to the overall simplicity of the antenna structure. Impedance in microstrip lines allows for easy management of the antenna system's impedance matching. The impedance can be tuned for optimal power transfer by altering the microstrip line widths, which is called a stepped impedance matching network. By separating the feed lines into various widths and sections, the antenna accomplishes balanced power distribution to the slots. The varied widths and segments of the feed lines will enable the design to manage impedance matching and power transfer to both slots, as shown in Figure 1 and Table 1. The use of two substrates in antenna design helps to provide increased isolation, symmetric feeding, regulated impedance, structural integrity, and overall antenna system performance improvement. Placing a substrate above the ground plane in the crossed-slot antenna design provides benefits such as dielectric loading, impedance matching, radiation enhancement, structural support, and regulated coupling, all of which contribute to the antenna's performance and usefulness.

Table 1: Value of Design Parameters

| No | Parameters | Symbol | Value(mm) |
|----|------------------------|--------|-----------|
| 1 | Substrate Width | Ws | 100 |
| 2 | Feed Length 1 | L1 | 3 |
| 3 | Substrate Thickness | Ts | 0.5 |
| 4 | Cross-Slot Length | Lc | 45 |
| 5 | Feed Line Length 5 | L5 | 17 |
| 6 | Feed Line Length 4 | L4 | 38 |
| 7 | Feed Line Length 3 | L3 | 10 |
| 8 | Feed Line Length 2 | L2 | 10 |
| 9 | Ground Thickness | Tg | 0.035 |
| 10 | Cross-Slot Width | Wc | 6.5 |
| 11 | Feed Width 50 Ω | W1 | 1.8 |
| 12 | Feed Line Width 2 | W2 | 0.75 |
| 13 | Feed Line Width 3 | W3 | 0.65 |
| 14 | Feed Line Width 4 | W4 | 0.65 |
| 15 | Feed Line Width 5 | W5 | 1.8 |
| 16 | Reflector Substrate | RL | 9 |
| 17 | Reflector Width | Rw | 130 |

2.2 Parametric studies

Numerous elements have been considered throughout the simulation optimization process, such as the microstrip line dimensions, cross-slot, ground width, and reflector width. Two important aspects will be thoroughly discussed: the microstrip line dimensions and the cross slot.

- 1) Microstrip line dimensions: To investigate the effect of key parameters, we compared the S11 and S12 parameters by varying the width of the feed line in relation to isolation and impedance matching. The results presented in Figures 2 and 3 and Table 1 indicate that altering the feed line width results in a gradual improvement in the S11 and S12 values. The aperture-coupling feed structure is a crucial design component in the creation of dual-polarized microstrip patch antennas for contemporary communication applications since it improves the antenna's overall performance in terms of bandwidth, isolation, and radiation pattern symmetry.
- 2) Cross-slot dimension: via altering the cross-slot dimension's width for impedance matching and isolation. The findings shown in Figures 4 and 5 and Table 2 show that the S11 and S12 values gradually improve as the cross-slot width is changed. For dual-polarized antennas, cross-slot configurations are employed to improve symmetrical far-field patterns and enhance port-to-port isolation. Consequently, the findings highlight the advantages of cross-slot structures in antenna design for antennas operating in the sub-6 GHz frequency band.

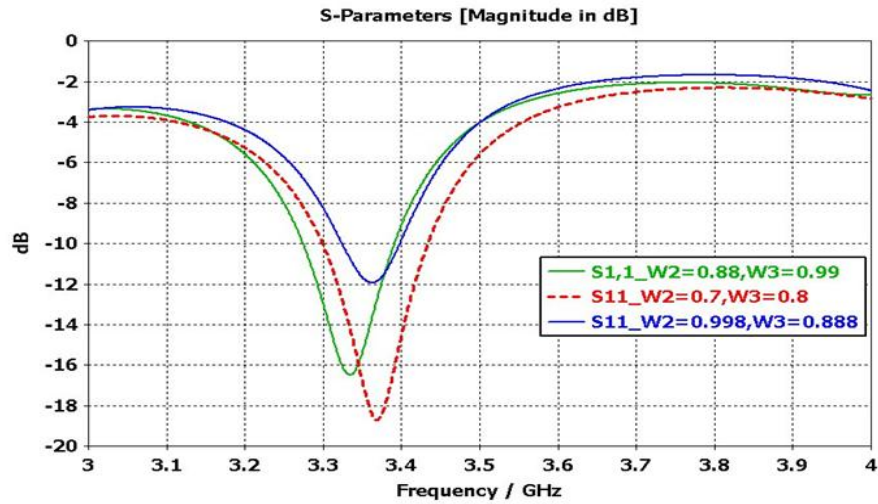


Figure 2: Evaluate the influence of feed line width on S11 parameters.

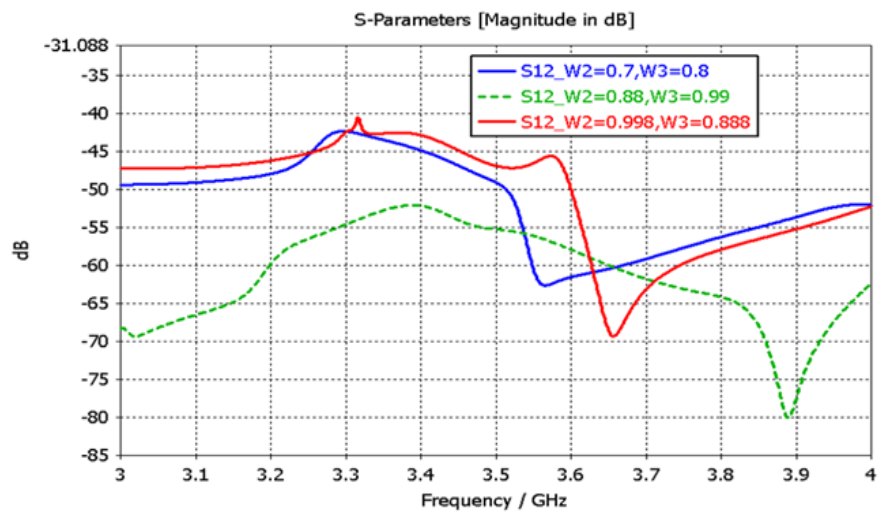


Figure 3: Evaluate the influence of feed line width on S12 parameters.

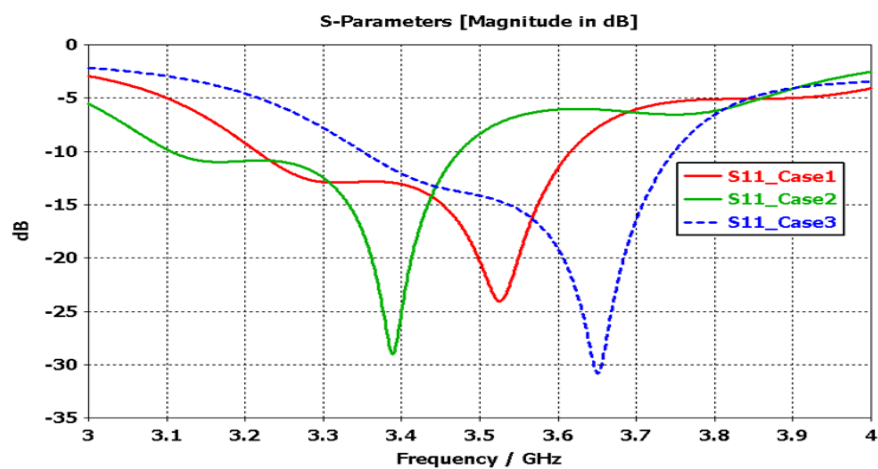


Figure 4: Evaluate the influence of cross slot width on S11 parameters.

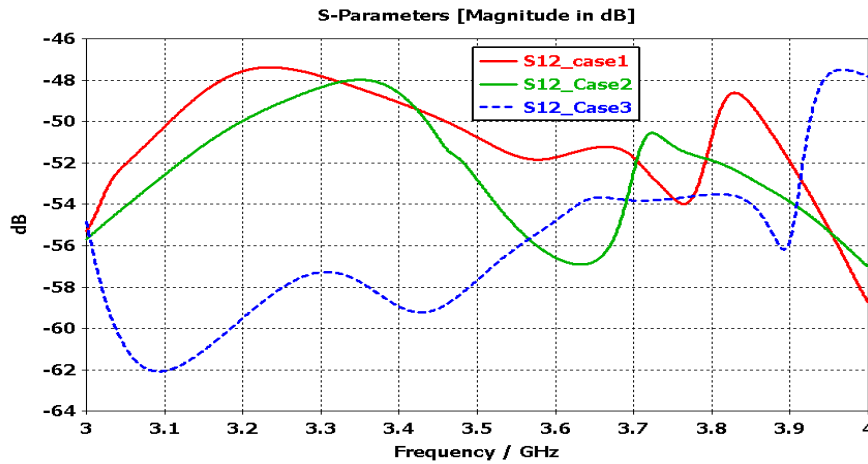


Figure 5: Evaluate the influence of cross-slot width on S12 parameters.

Table 2: The parameters for the effect of cross slot dimension on S-parameters

| Cases | W2(mm) | W3 (mm) | Wc(mm) | Lc(mm) |
|-------|--------|---------|--------|--------|
| Case1 | 0.998 | 0.888 | 4 | 30 |
| Case2 | 0.998 | 0.888 | 4 | 30 |
| Case3 | 0.88 | 0.77 | 3 | 28 |

2.3 Results of Single Element Optimization

Figure 6 and Table 3 represent all the optimized parameters performed by CST Microwave Studio 2020, covering a wide bandwidth for a better than $S_{11} = -15$ dB, isolation less than -50, VSWR = 1.4, and impedance bandwidth of 19.72% (3.2-3.9 GHz). S_{11} of better than -15 dB is normally recommended for antenna elements used in base transceiver stations due to the requirement of connection to the radio unit. Assuming that the bandwidth for S_{11} of better than -10 dB results in a higher bandwidth. The results cover more than the n78 band for sub-6 GHz 5G applications.

The radiation pattern properties at the first, middle, and end edges of the bandwidth are shown in Figure 7 and Figure 8. They represent the E-plane, H-plane, and slant 45-degree radiation patterns of the antenna, which are plotted in both perpendicular radiations. Both copolar and cross-polar patterns are shown and are overlaid. For the first frequency (3.1 GHz), the antenna has a gain of 8.5 dBi; for the second frequency (3.5 GHz), it has a gain of 7 dBi; and for the third frequency (3.9 GHz), it has a gain of 10.5 dBi. As a result, isolation purity is outstanding across a broad spectrum and remains reasonable in most forward directions. One important point is that when we plot the orthogonal radiation patterns of the normal structure at the E-plane and H-plane, they are not identical. However, in such a case, the ± 45 degree radiation patterns of the elements are identical and balanced. This proves that if we rotate the antenna structure by 45 degrees, then the radiation patterns of the antenna at the E-plane and H-plane are identical.

In the following section, we will address the array of dual-polarized antennas. However, before that, it is essential to discuss ground radiation, as it plays a significant and influential role in antenna design. We will explore this topic from both mathematical and practical perspectives.

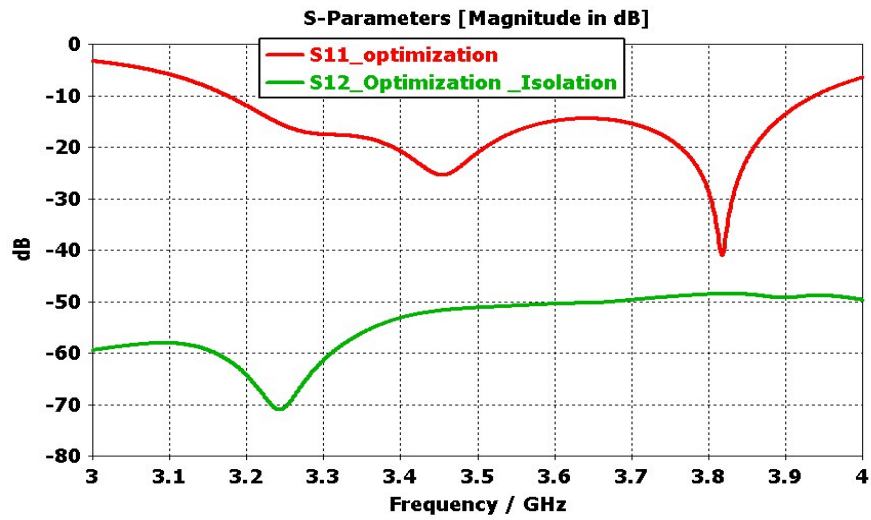
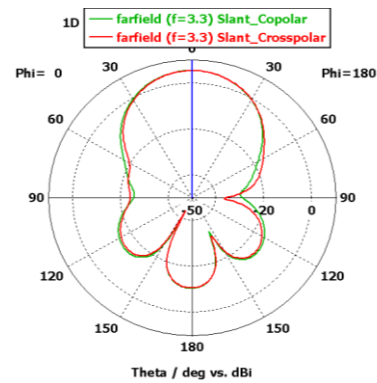
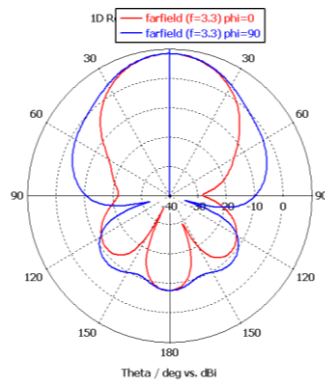


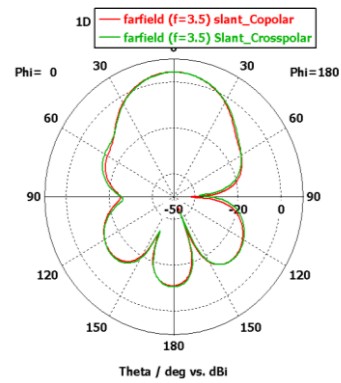
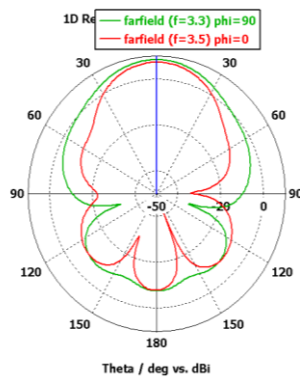
Figure 6: The S11 and S12 obtained by optimizing all parameters

Table 3: Evaluate the optimization of all parameters

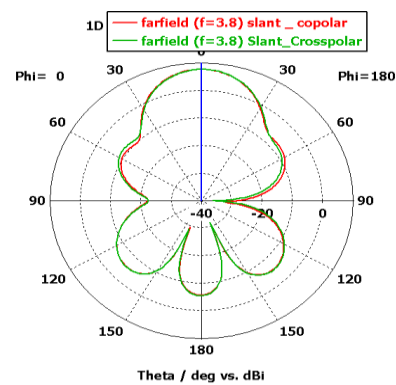
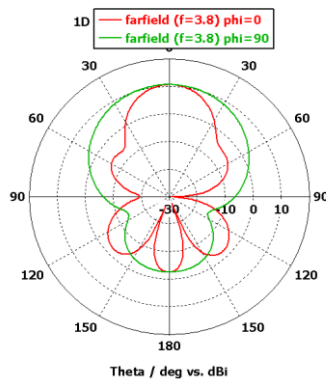
| No | Column A | Symbol | Value(mm) |
|----|------------------------|--------|-----------|
| 1 | Substrate Width | Ws | 80 |
| 2 | Feed Length 1 | L1 | 5.52 |
| 3 | Substrate Thick | Ts | 0.5 |
| 4 | Cross-Slot Length | Lc | 28.9 |
| 5 | Feed Line Length 5 | L5 | 15.82 |
| 6 | Feed Line Length 4 | L4 | 32 |
| 7 | Feed Line Length 3 | L3 | 7.77 |
| 8 | Feed Line Length 2 | L2 | 9.48 |
| 9 | Ground Thickness | Tg | 0.035 |
| 10 | Cross-Slot Width | Wc | 3.41 |
| 11 | Feed Width 50 Ω | W1 | 1.62 |
| 12 | Feed Line Width 2 | W2 | 0.8 |
| 13 | Feed Line Width 3 | W3 | 0.851 |
| 14 | Feed Line Width 4 | W4 | 0.851 |
| 15 | Feed Line Width 5 | W5 | 1.828 |
| 16 | Reflector Substrate | RL | 11.76 |
| 17 | Reflector Width | Rw | 100 |

Linear polarization: Vertical & HorizontalSlant 45degree polarization: Copolar & Xpolar

(a)



(b)



(c)

Figure 7: Simulated far-field radiation patterns of the single element for the linear vertical/horizontal polarization case versus the slant case. (a) at 3.3 GHz, (b) at 3.5 GHz, (c) at 3.8 GHz

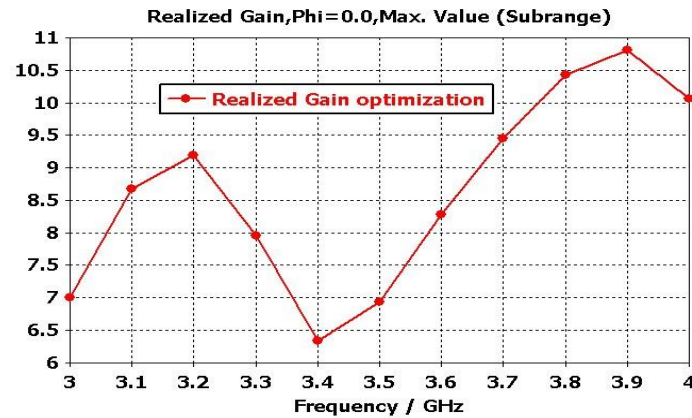


Figure 8: The Gain for optimizing all parameters

3 Ground Radiation Issue

Unfortunately, our cross-slot antenna structure has a rectangular patch mode as well. A rectangular patch antenna can be depicted as an array of two radiating narrow apertures (slots), each with a width W and height h , separated by a distance L as shown in Figure 9 below. The portion of the main radiation should occur from these two grounds back slots; call it slot mode. However, other possible modes of radiation should be suppressed and kept controlled. Surface wave mode and patch mode are two of them; the latter is more significant. In fact, the latter is dominant when the resonant frequency of the patch mode is close to that of the slots. The patch mode is the radiation that directly comes from the edges of the upper ground. In fact, the ground and the reflector of the main antenna form a patch antenna.

The level of fringing radiation from the patch mode is determined by the patch dimensions and the substrate height. The fringing in the primary E plane (xy plane) depends on the ratio of patch length L to substrate height h ($\frac{L}{h}$) and substrate dielectric constant ϵ_r . Patch antennas have less fringing ($L/h \gg 1$), although it still affects the antenna resonance frequency and width. Most of the electric field lines are located in the substrate, with portions of some lines in the air. As $W/h \gg 1$ and $\epsilon_r \gg 1$, the electric field lines primarily concentrate in the substrate. In this scenario, fringing makes the microstrip line appear electrically wider than its physical size.

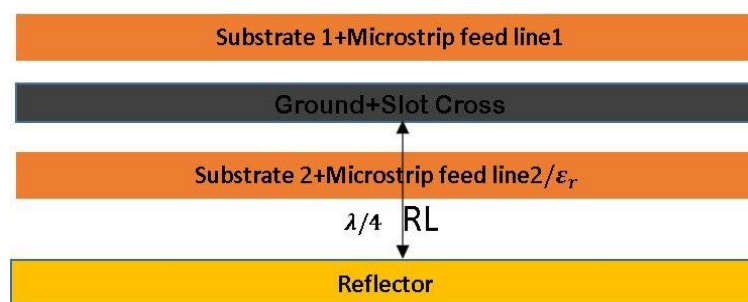


Figure 9. The ground and the reflector of the cross-slot antenna

Many parameters affect the fringe fields of a rectangular patch antenna, including patch dimensions (L and W), substrate height (h), dielectric constant (ϵ_r), effective dielectric constant (ϵ_{eff}), operating frequency, ground plane size, and edge effects. The patch dimensions have been expanded on each end by a distance ΔL , which is a function of the effective dielectric constant (ϵ_{reff}) and width-to-height ratio (W/h). The length extension due to fringing fields (ΔL) (Balanis, 2016):

$$\Delta L = 0.42 h \frac{(\epsilon_{eff} + 0.3)(\frac{w}{h} + 0.264)}{(\epsilon_{eff} - 0.258)(\frac{w}{h} + 0.8)} \quad (1)$$

$$\epsilon_{eff} = \frac{\epsilon_r + 1}{2} + \frac{\epsilon_r - 1}{2} \left(1 + 12 \frac{h}{w}\right)^{-1/2} \quad (2)$$

The effective length (L_{eff})

$$L_{eff} = L + 2\Delta \quad (3)$$

The resonant frequency of a rectangular patch antenna depends on its length. Typically, it is given by accounting for fringing; however, it should be updated to add edge effects and computed using

$$f_{fringing} = \frac{1}{2L_{eff} \sqrt{\epsilon_{eff}} \sqrt{\mu_0 \epsilon_0}} = \frac{1}{2(L + 2\Delta) \sqrt{\epsilon_{eff}} \sqrt{\mu_0 \epsilon_0}} = \frac{c}{2(L + 2\Delta) \sqrt{\epsilon_{eff}}} \quad (4)$$

$$f_{fringing} = R \frac{c}{2L \sqrt{\epsilon_{eff}}} \quad (5)$$

Where the permittivity $\mu_0 = 1.26 \times 10^{-6}$, permeability $\epsilon_0 = 2.997 \times 10^{-12}$, velocity of light $c = \frac{1}{\sqrt{\mu_0 \epsilon_0}} = 2.997925 \times 10^8$ m/s, fringing factor $R = \frac{1}{(1+2\Delta L)}$.

The ground plane should be large enough to support proper radiation but not excessively large to avoid unwanted reflections and surface waves. A typical ground plane size is about $\lambda/2$ larger than the patch dimensions on all sides. The patch is placed above a ground plane, with the reflector below to enhance directivity. The first resonant frequency is approximately 1.875 GHz, and the second resonant frequency is 3.75 GHz. The radiation pattern of the patch at its second resonant frequency in this mode differs from that of the radiation slot; therefore, the mode exhibits a null in the broadside direction of the antenna. We need to modify the antenna shape to maintain the beam shape and match the enlargement of the ground base. In Figure 10, we observe that the E-field does not propagate from the cross slot, but rather from the edges of the antenna, which makes the field non-circular.

The paper discusses the use of an operation frequency of 3.5 GHz and the $\lambda \approx 85.7$ mm. The ground plane should extend approximately 42.85 mm beyond the edges of the patch elements.

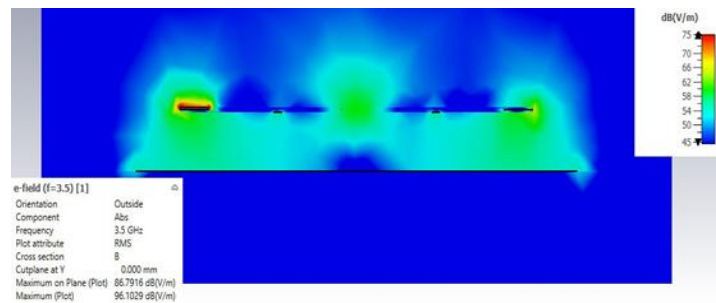


Figure 10: The E-field radiation at the center frequency of 3.5 GHz without pins

Adding steel pins between the reflector and the ground plane can help to lessen the quasi-cavity effects. This method is also known as employing pin arrays or "electromagnetic bandgap (EBG) structures" to suppress surface waves and undesirable resonances.

In Figure 11, Surface waves can enhance the quasi-cavity effect by providing extra routes for electromagnetic

radiation to reflect and interfere. The pins effectively change the impedance characteristics of the ground and reflector. This may reduce the production of standing waves and resonances. The pins can absorb and disperse some of the electromagnetic energy, reducing the constructive interference patterns that lead to the quasi-cavity effect.

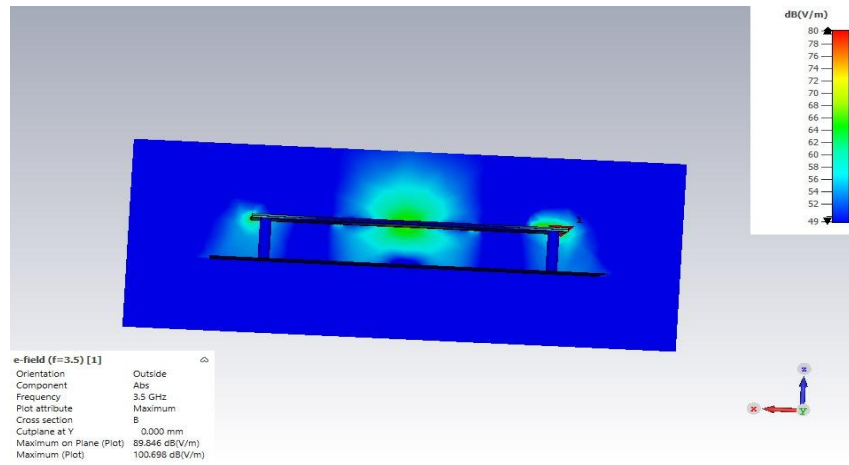


Figure 11: The effect of conductive short circuit pins to limit radiation at the center frequency of 3.5 GHz

4 Array of Dual-Polarized Configuration

In this paper, we need to design a 2x1 subarray microstrip patch antenna at a given frequency, such as 3.5 GHz, which can be difficult, especially when dealing with ground plane size and radiation pattern. The array configuration of dual-polarized antennas is the organization of several antenna elements to achieve certain performance goals, such as enhanced gain, beamforming, diversity, or pattern shaping. Designing a 2x1 subarray microstrip patch antenna at a specific frequency, such as 3.5 GHz, can be difficult, especially when dealing with a power divider, ground plane size, and radiation pattern. As a result, in this section, we will discuss two significant aspects that are worth researching in order to get better results: power dividers and mutual coupling.

4.1 Power Divider

Power dividers are an important part of array antenna design by dividing the input signal into several output ports with specific amplitude and phase characteristics. Array antenna systems typically use a variety of power dividers, including Wilkinson, T-junction, hybrid coupler, corporate feed network, and series feed network. But we chose the T-junction power divider because of its simplicity and straightforward design, which divides incoming power evenly or unequally into two or more output ports based on the rules discussed in (Pozar, 2012). It is widely used in basic RF and microwave circuits because of its simplicity and ease of construction. To match the divider to the input line with characteristic impedance z_0 , we must

$$Y_{in} = \frac{1}{z_0} = \frac{1}{z_1} + \frac{1}{z_2} + j\beta \quad (6)$$

If the transmission lines are believed to be lossless, then the characteristic impedances are real; additionally, we assume $\beta = 0$, so (5) reduces to

$$\frac{1}{z_0} = \frac{1}{z_1} + \frac{1}{z_2} \quad (7)$$

In total, we need four equal power dividers in the 1 by 2 subarray. We have already used two of them in a single-element design to excite each slot. However, two more dividers are needed to form the two-element array.

Figure 12 shows one of the power dividers designed to match the 30Ω input impedance of each element, Z_1 and Z_2 , to 15Ω , which is the input impedance of the array.

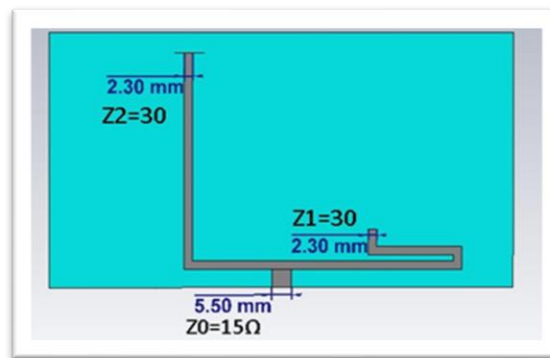


Figure 12: Transmission line model of the lossless T-junction divider used in this design

4.2 Mutual Coupling

Several techniques are available to reduce mutual coupling, including electromagnetic shielding, electromagnetic bandgap structures, reconfigurable antennas, antenna decoupling, impedance matching networks, baluns, filters, defective ground structures, and metal vias. But in this paper, we used the type of metal via because it does not affect the figure and geometry of the antenna. The proposed approach employs a defect ground structure (DGS) and metal vias. The DGS is put between the patch antennas to improve isolation and reduce coupling between them. Metal vias link the DGS to the ground plane, further improving isolation (Guo et al., 2021). The DGS can be thought of as a series of resonant slots or forms carved into the ground plane to form a band-stop filter that blocks or attenuates specific frequencies. Placing a DGS underneath a microstrip antenna allows you to suppress undesired radiation, reduce mutual coupling between antennas, and improve impedance matching. The vias are designed to connect the DGS to the ground plane, creating a low-impedance path for the surface currents induced by the patch antennas. This helps to reduce the mutual coupling between the patch antennas and increase the isolation between them (Bisharat et al., 2016).

4.3 Array Result for Different Scenarios

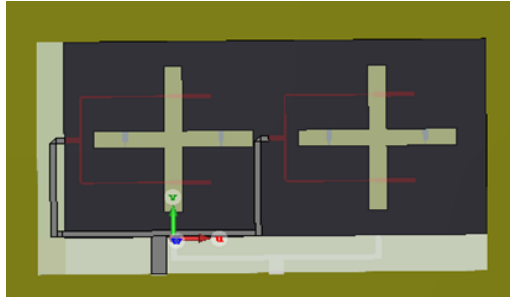
The designed dual-polarized antenna has been put in a two-element array in two cases: 1) Vertical/horizontal polarization 2) $\pm 45^\circ$ slant polarization. The radiation pattern in both cases has been studied and reported in the following.

4.4 Vertical/Horizontal Polarization Case

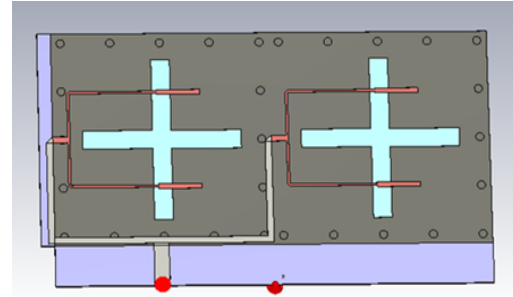
As depicted in Figure 13, the linear vertical/horizontal two-element array is created twice: once with the via pins and once without them. In the without-via case, the S_{11} is below -10 dB from 3.25 to 3.7 GHz (450 MHz). Additionally, the S_{11} is below -10 dB from 3.1 to 3.5 GHz (400 MHz) with the via. The gain is reported as 13.5 dBi, both with and without a via. We observe that the gain has significantly improved from 10.5 dBi in a single optimized antenna to 13.5 dBi in a two-element linear array. As can be seen, the results show that the mutual coupling deteriorates the radiation pattern with the side lobe of around -12.6 dB at 3.4 GHz. However, the side lobe level is better at the level of -19 dB, although not acceptable in the case of a square via. Additionally, the side lobe in the linear horizontal configuration is approximately -18.4 dB at 3.4 GHz without a via, while it improves slightly to around -19 dB with a via. However, $VSWR < 1.5$ for all cases. The structural Dual polarization integration and electromagnetic performance of multilayer or aperture-coupled antennas are enhanced when pin vias are included in antenna design. It enhances isolation in dual-polarized structures, lessens mutual coupling between radiating components, and suppresses the propagation of surface waves. They also minimize

undesired parasitic radiation and improve bandwidth stability by offering a dependable ground connection between the antenna's layers.

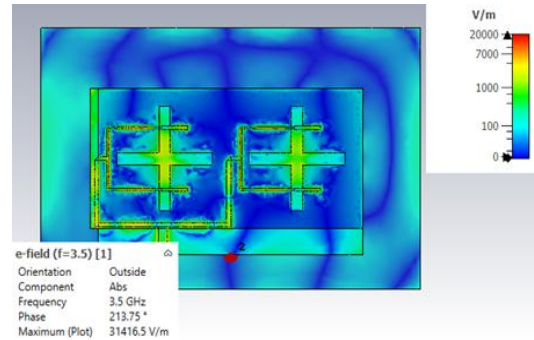
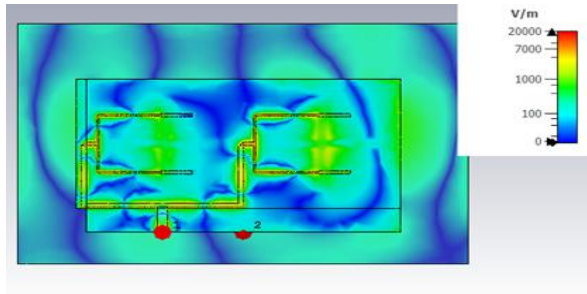
Without via



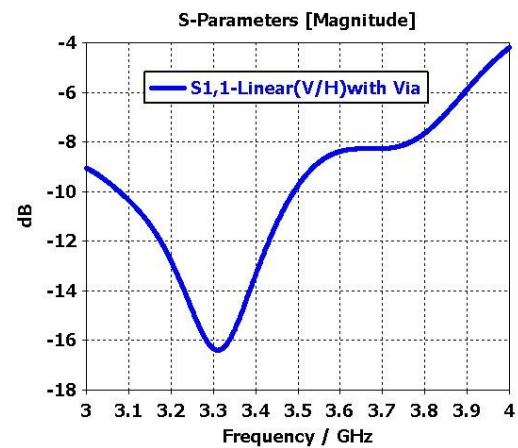
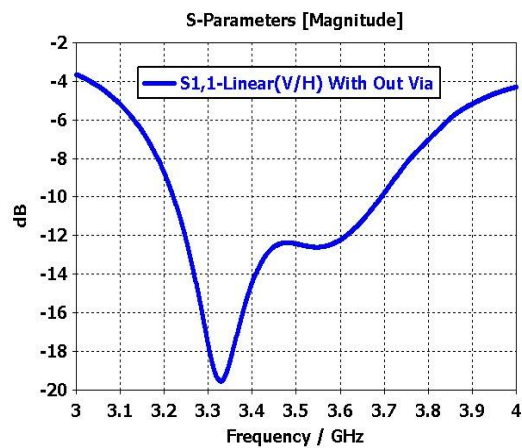
With via



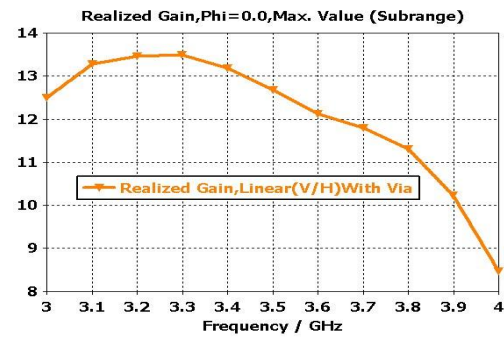
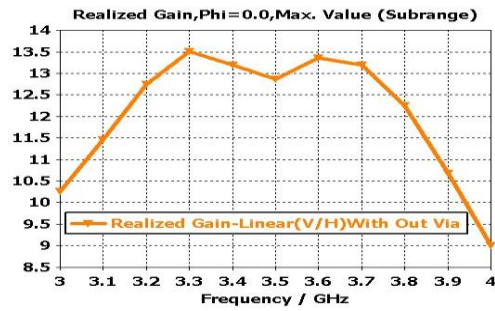
(a)



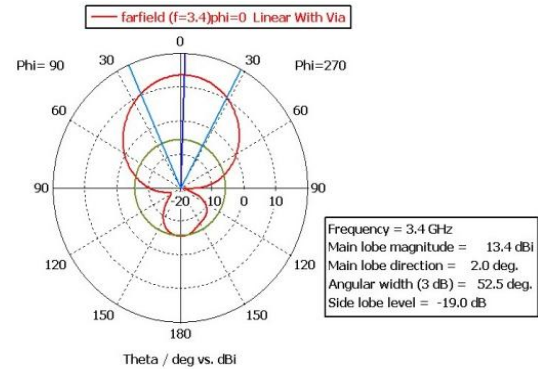
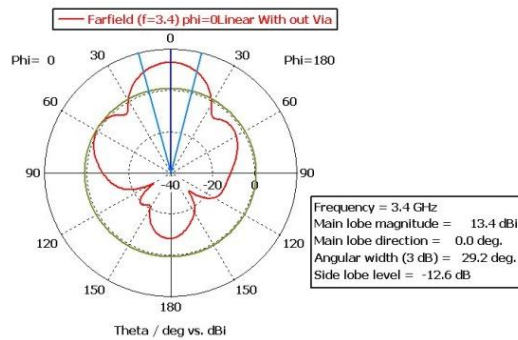
(b)



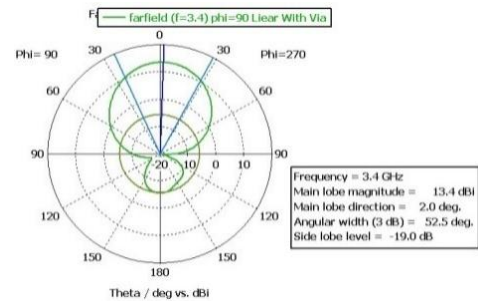
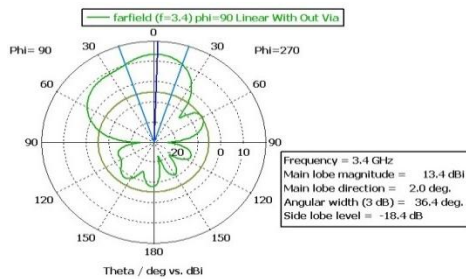
(c)



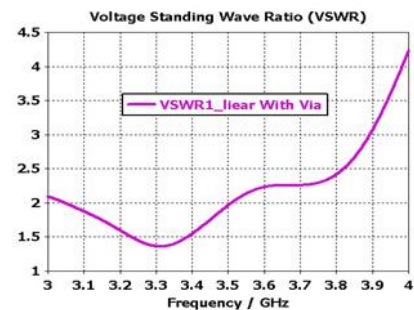
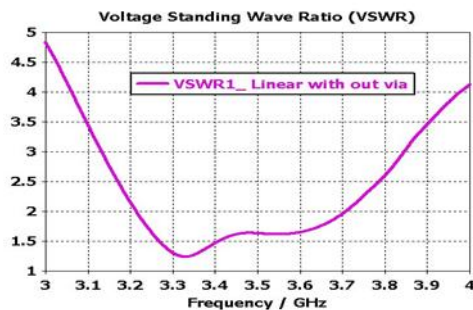
(d)



(e)



(f)

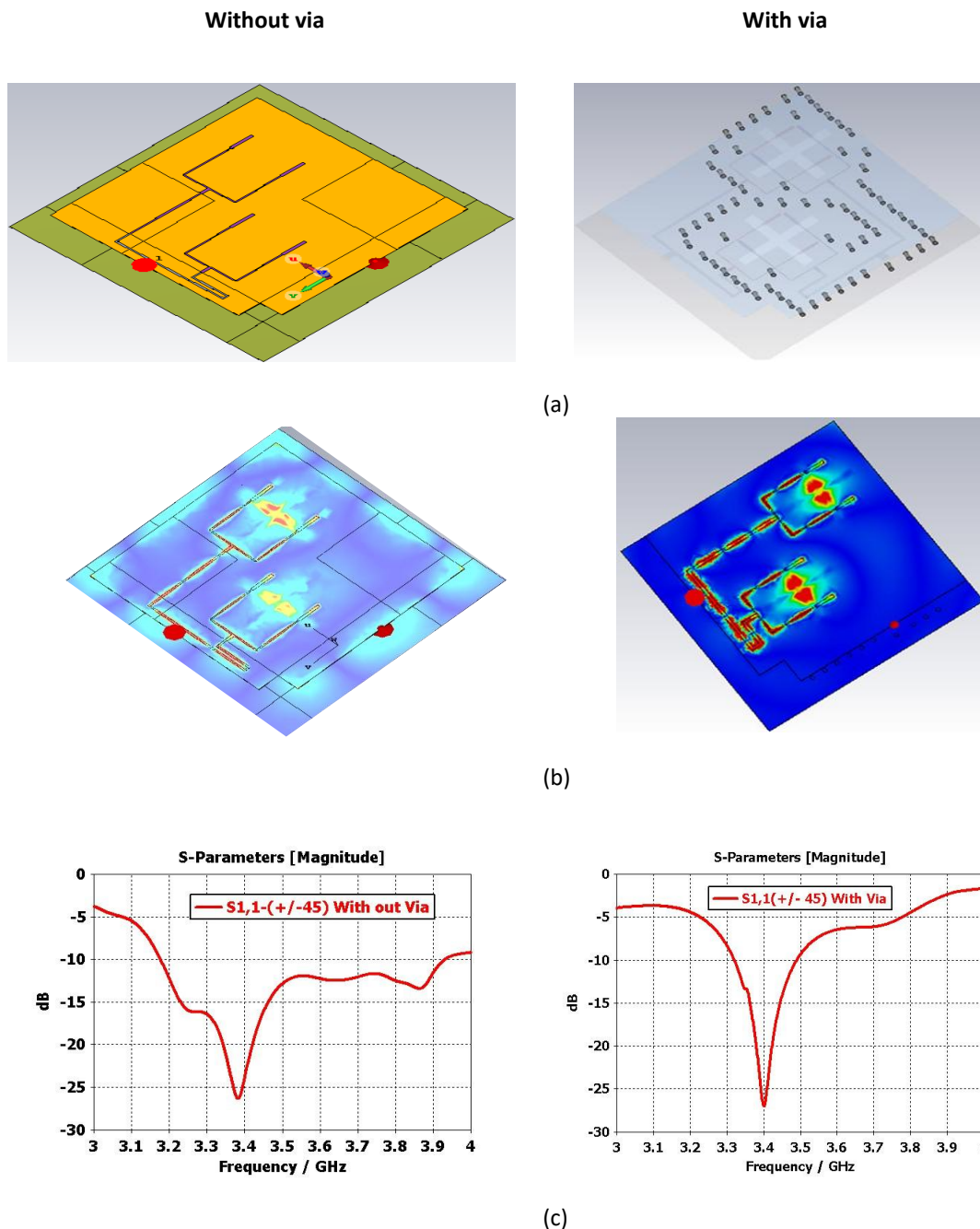


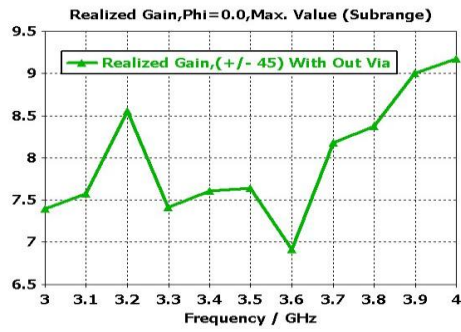
(g)

Figure 13: Two-element array vertical/horizontal Polarization without via and with via; (a) two-element array, (b) E-field distribution from the cross-slot array at 3.5 GHz, (c) BW (3.25-3.7 GHz), (d) Gain=13.5 dB, (e) Radiation pattern far-field at 3.4 GHz, side lobe -12.6 dB at $\phi=0$, (f) Radiation pattern far-field at 3.4 GHz, side lobe -18.4 dB at $\phi=90$, (g) VSWR <1.5.

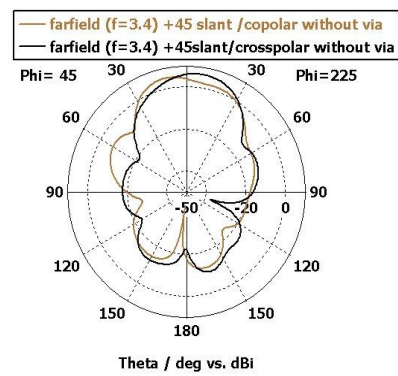
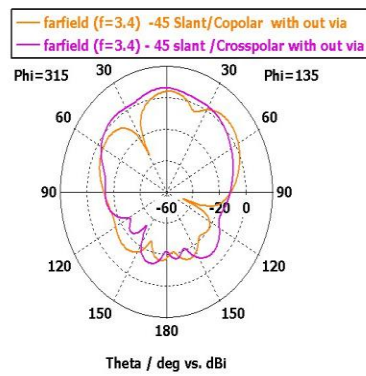
4.5 $\pm 45^\circ$ Slant Polarization

The two-element array $\pm 45^\circ$ slant polarization is produced once with and once without the via pins, as seen in Figure 14. In the absence of a via, the S_{11} is below -10 dB from 3.2 to 3.9 (700 MHz), and the S_{11} is below -10 dB from 3.3 to 3.5 GHz (200 MHz) with a via. The gain is 9 dBi for both scenarios; additionally, the VSWR is less than 1.5 in both cases. The 45 -degree slant radiation patterns of the antenna, which are plotted in both perpendicular radiations. Both Copolar and cross-polar patterns are shown and are overlaid. The observed decrease in bandwidth for the slanted $\pm 45^\circ$ antenna array with vias is ascribed to parasitic effects brought about by the vias, which deteriorate impedance matching by introducing extra capacitance and inductance. The basic resonant frequency of the antenna is lowered by this parasitic capacitance. In order to restore resonance to the desired frequency, you probably had to decrease the patch size. However, doing so prevents the design from remaining inside the sub-6 GHz region.

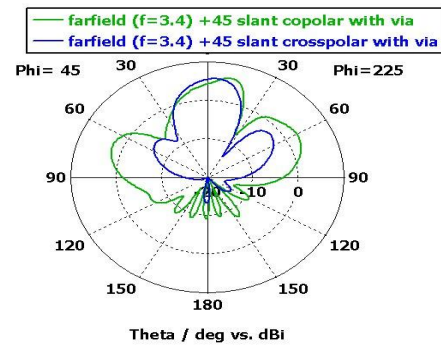
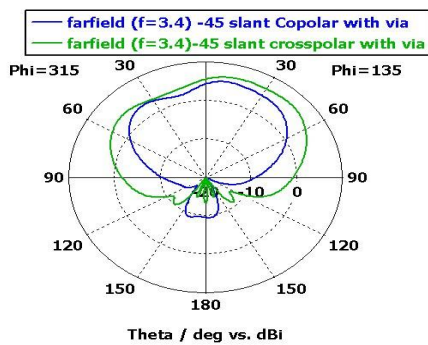




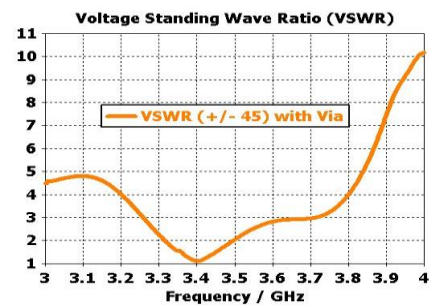
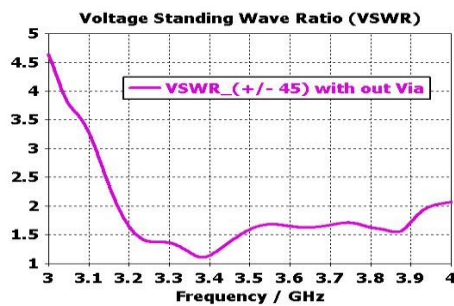
(d)



(e)



(f)



(g)

Figure 14: Two-element array ± 45 degrees without via and with via; (a) Two-Element Array $2 \times 1 \pm 45$ degree, (b) E-field distribution on the ground, (c) BW, (d) The gain is 9 dBi, (e) far-field radiation (-45) slant Copolar and crosspolar at 3.4 GHz, (f) far-field radiation (-45) slant Copolar and crosspolar at 3.4 GHz, (g) VSWR.

Summary table 4 has been included to help make the comparison between the suggested design and other configurations more understandable. The -10 dB impedance bandwidth (IBW%), realized gain (dBi), isolation (dB), and frequency bands are among the important performance indicators for each specified antenna configuration that are highlighted in this table. The comparison illustrates how structural differences, including via existence or absence and polarization orientation (linear vs. slant $\pm 45^\circ$), affect the overall characteristics and electromagnetic performance of the antennas utilized for Sub-6 GHz 5G applications. Additionally, as summarized in Table 5, the literature compares the proposed cross-slot antenna with earlier works, indicating that this antenna design proposal is a strong competitor to other shapes, such as the aperture-coupled design, which is known for its broad impedance bandwidth.

Table 4: Comparison between the suggested design and other configurations

| Antenna Configuration | Worst Isolation dB | Antennas Structure | -10 dB IBW% | Average Gain dBi | Frequency Band(GHz) |
|---------------------------------------|--------------------|--------------------|--------------|------------------|---------------------------|
| Single Antenna Optimization | 50 | Crossed Slot | 19.72 | 11.7 | 3.2-3.9 |
| Two Antenna(V/H) without via | -22 | Crossed slot | 34 | 13.5 | (3.15-3.57) |
| Two Antenna (V/H) with Via | -28 | Crossed slot | 28.6 19.7 | 11.5 | (3.26-3.43) |
| Two Antenna (± 45) with Out via | -12 | Crossed slot | 68 | 11.3 | 3.134-3.550 3.737-3.98 |
| Two Antenna (± 45) with via | -50 | Crossed slot | 11.4 28.3 | 10 | 3.3-3.7 1.71-2.2 |

Table 5: compared the proposed cross-slot antenna with earlier works

| The Antenna References | Isolation dB | Antennas Structure | -10 dB IBW% | Average gain dBi | Frequency Band(GHz) |
|------------------------|---------------------------|---|----------------|------------------|---------------------------|
| Vaziri et al. (2013) | 35 | coupled microstrip patch | 24 | 9.2 | 4-6.5 |
| Chen et al. (2013) | 60 | Crossed slot | 34 | 8.5 | 4-4.7 |
| Sun et al. (2019) | 30 | cross-band scattering | 28.6 19.7 | 11.5 10 | 1.7-2.7 0.82-1 |
| Zhang & Gao (2018) | 20 | crossed bow-tie dipole | 68 | 8 | 1.427-2.9 |
| Sun et al. (2020) | 26 | spiral-choke | 11.4 28.3 | 11 | 3.3-3.7 1.71-2.2 |
| Ding et al. (2021) | 9.3 | Sparse phased / null scanning | 2.3 | 8 | 2.52-2.58 |
| Zhang et al. (2023) | not applicable | Reconfigurable meta surface/Varactor Diodes | 11.5 | (no active feed) | 9.8-11 |
| Azari et al. (2023) | 12 | bowtie patch | 57.8 | 7 | 24-43.5 |
| Azari et al. (2024) | 30 | aperture-coupled | 21 | 7 | 24-44 |
| Tabaiya et al. (2025) | no port-to-port isolation | H-shaped Grid-Meta surface | 15.45 13.63 | 6 | 5.81- 6.78 4.31 - 4.94 |
| This Work | 50 | Cross-Slot | 19.72 | 11.7 | 3.2-3.9 |

5 Conclusion

In this research, an array antenna for a dual linear polarized antenna with high isolation and broadband at sub-6 GHz 5G is designed. For the antenna to work with the array base station, several parameters are optimized to achieve a better result, such as isolation, gain, and bandwidth. The results showed high gain (7 dBi to 10.5 dBi), very high isolation (better than -50 dB), and a 19.72% (3.2-3.9 GHz) wide bandwidth for the reflection coefficient of better than -15 dB. A two-element array is formed once with and once without the via pins in two cases: 1-vertical/horizontal polarization. 2- $\pm 45^\circ$ slant polarization was studied and designed. We prove that the presence of vias also makes the matching more problematic because some of the undesirable radiating modes are blocked from radiation in the first case. Consequently, this leads to improvements in bandwidth and gain. In case two, the basic resonant frequency of the two antennas is lowered by this parasitic capacitance, so we need to decrease the patch size, and doing this will prevent the design from remaining inside the sub-6 GHz region. This phenomenon explains the decrease in bandwidth. These results validate that the suggested structure is appropriate for contemporary beamforming and MIMO systems. The results obtained and the compatibility achieved in this direction allow for the possibility of using this antenna in many applications in modern communications systems, such as advanced antenna systems (AAS) and radars.

Acknowledgment

The authors would like to thank MCI Hamrah Aval for their support of this work.

Conflict of interest

The authors declare that there are no conflicts of interest regarding the publication of this manuscript

References

- Asplund, H., Karlsson, J., Kronestedt, F., Larsson, E., Astely, D., von Butovitsch, P., ... & Jöngren, G. (2020). Advanced antenna systems for 5G network deployments: bridging the gap between theory and practice, Academic Press.
- A. Azari, J A. K. Skriversvik, S. and H. Aliakbarian, Mar. (2023). Design methodology for wideband bowtie patch antenna for 5G mm Wave applications, in *Proc. 17th Eur. Conf. Antennas Propag. (EuCAP)*, Florence, Italy, pp. 1–4, doi: 10.23919/EuCAP57121.2023.10132909
- A. Azari, J A. K. Skriversvik, S. and H. Aliakbarian, (2024). A mm Wave Low Complexity and Low-Cost Super Wideband Dual-Polarized Aperture Coupled Antenna for 5G Applications, *IEEE Access*, doi: 10.1109/ACCESS.2024.3415167.
- Balanis, C.A. (2016). 'Antenna theory: analysis and design ', John wiley & sons.
- Chen, Y. and Vaughan, R.G. (2013). Crossed slot antenna with simple feed for high polarization isolation, *IEEE Antennas and Propagation Society International Symposium (APSURSI)*, pp. 650-651, doi: 10.1109/APS.2013.6710985.
- Dia'aaldin, J. B., Liao, S., and Xue, Q. (2015). *High gain and low cost differentially fed circularly polarized planar aperture antenna for broadband millimeter-wave applications*, *IEEE Transactions on Antennas and Propagation*, 64(1), pp. 33–42, <https://doi.org/10.1109/TAP.2015.2499750>
- Ding, Z., Chen, J., Liu, H., He, C., and Jin, R. (2021). *Grating lobe suppression of sparse phased array by null scanning antenna*, *IEEE Transactions on Antennas and Propagation*, 70(1), pp. 317–329, doi: 10.1109/TAP.2021.3090573.
- Gao, S., Li, L. W., Leong, M. S., and Yeo, T. S. (2003). *A broadband dual-polarized microstrip patch antenna with aperture coupling*, *IEEE Transactions on Antennas and Propagation*, 51(4), pp. 898–900, doi: <https://doi.org/10.1109/TAP.2003.814795>

- Guo, Y. J. and Ziolkowski, R. W. (2021). *Advanced antenna array engineering for 6G and beyond wireless communications*. John Wiley & Sons.
- Huang, Y. H., Wu, Q., and Liu, Q. Z. (2009). *Broadband dual-polarised antenna with high isolation for wireless communication*, Electronics Letters, 45(14), pp. 714–715, doi: <https://doi.org/10.1049/el.2009.1586>
- Jeon, J. S. (2011). *Design of wideband dual-polarized microstrip antennas*, URSI General Assembly and Scientific Symposium, pp. 1–4, doi: 10.1109/URSIGASS.2011.6050296.
- Li, B., Yin, Y. Z., Hu, W., Ding, Y., and Zhao, Y. (2012). *Wideband dual-polarized patch antenna with low cross polarization and high isolation*, IEEE Antennas and Wireless Propagation Letters, 11, pp. 427–430. <https://doi.org/10.1109/LAWP.2011.2176093>
- Muirhead, D., Imran, M. A., and Arshad, K. (2016). *A survey of the challenges, opportunities and use of multiple antennas in current and future 5G small cell base stations*, IEEE Access, 4, pp. 2952–2964. <https://doi.org/10.1109/ACCESS.2016.2569483>
- Pozar, D. M. (2012). *Microwave engineering*, 4th ed., John Wiley & Sons.
- Sun, H. H., Ding, C., Zhu, H., Jones, B., and Guo, Y. J. (2019). *Suppression of cross-band scattering in multiband antenna arrays*, IEEE Transactions on Antennas and Propagation, 67(4), pp. 2379–2389. <https://doi.org/10.1109/TAP.2019.2897865>
- Sun, H. H., Zhu, H., Ding, C., Jones, B., and Guo, Y. J. (2020). *Scattering suppression in a 4G and 5G base station antenna array using spiral chokes*, IEEE Antennas and Wireless Propagation Letters, 19(10), pp. 1818–1822. <https://doi.org/10.1109/LAWP.2020.3011699>
- Sun, H. H., Jones, B., Guo, Y. J., and Lee, Y. H. (2020). *Suppression of cross-band scattering in interleaved dual-band cellular base-station antenna arrays*, IEEE Access, 8, pp. 222486–222495. <https://doi.org/10.1109/ACCESS.2020.3041232>
- Tabaiya, K., Thitimahatthanakusol, P., Konpang, J., and Supreeyattitkul, N. (2025). *Dual-band same-sense circularly polarized grid-metasurface antenna for C-band spectrum utilization*, International Electrical Engineering Congress (iEECON), pp. 1–4, doi: 10.1109/iEECON64081.2025.10987781.
- Zhang, Q. and Gao, Y. (2018). *A compact broadband dual-polarized antenna array for base stations*, IEEE Antennas and Wireless Propagation Letters, 17(6), pp. 1073–1076. <https://doi.org/10.1109/LAWP.2018.2846521>
- Zhang, Y., Li, Y., and Zhou, Y. (2023). *Reconfigurable metasurface with varactor diodes for dynamic beam scanning in X-Band*, IEEE International Workshop on Electromagnetics: Applications and Student Innovation Competition (iWEM), pp. 84–86, doi: 10.1109/iWEM58222.2023.10234886.
- Vaziri, A., Kaboli, M., and Mirtaheri, S. A. (2013). *Dual-polarized aperture-coupled wideband microstrip patch antenna with high isolation for C-Band*, Iranian Conference on Electrical Engineering (ICEE), pp. 1–4. doi: 10.1109/IranianCEE.2013.6599842.